# Development of an efficient, ready to use, blood platelet-release device based on two new flow regime parameters: The periodic hydrodynamic loading and the shear stress accumulation.

Anaïs Pongérard, Léa Mallo, Valentin Do Sacramento, Olivier Boiron, Anita Eckly, Christian Gachet, François Lanza, Yannick Knapp, Catherine Strassel

New BIOTECHNOLOGY 77 (2023) 68–79

Contents lists available at ScienceDirect

New BIOTECHNOLOGY

journal homepage: www.elsevier.com/locate/nbt

# Development of an efficient, ready to use, blood platelet-release device based on two new flow regime parameters: The periodic hydrodynamic loading and the shear stress accumulation.

Anaïs Pongérard [a], Léa Mallo [a], Valentin Do Sacramento [a], Olivier Boiron [b], Anita Eckly [a], Christian Gachet [a], François Lanza [a], Yannick Knapp [c], Catherine Strassel [a,*]

[a] Université de Strasbourg, INSERM, EFS Grand-Est, BPPS UMR-S1255, FMTS, F-67065 Strasbourg, France
[b] CNRS, Université Aix-Marseille, Ecole Centrale Marseille, IRPHE UMR7342, F-13000 Marseille, France
[c] Université Avignon, LAPEC UPR-4278, F-84000 Avignon, France

ARTICLE INFO

*Keywords:*
Cultured platelets
Flow regime
Large-scale production
Shear stress accumulation

ABSTRACT

*In vitro* production of blood platelets for transfusion purposes is gaining interest. While platelet production is now possible on a laboratory scale, the challenge is to move towards industrial production. Attaining this goal calls for the development of platelet release devices capable of producing large quantities of platelets. To this end, we have developed a continuous-flow platelet release device composed of five spherical chambers each containing two calibrated cones placed in a staggered configuration. Following perfusion of proplatelet-bearing cultured megakaryocytes, the device achieves a high yield of about 100 *bona-fide* platelets/megakaryocyte, at a flow rate of ~80 mL/min. Performances and operating conditions comply with the requirements of large-scale platelet production. Moreover, this device enabled an in-depth analysis of the flow regimes through Computational Fluid Dynamics (CFD). This revealed two new universal parameters to be taken into account for an optimal platelet release: i.e. a periodic hydrodynamic load and a sufficient accumulation of shear stress. An efficient 16 Pa.s shear stress accumulation is obtained in our system at a flow rate of 80 mL/min.

## Introduction

Blood platelets are key players in bleeding arrest. To sustain an average count of $3 \times 10^{11}$ platelets/L of blood in Man, $10^{11}$ functional platelets are produced daily from their medullar precursors, the megakaryocytes (MK). Transfusion of platelet concentrates (PC) containing $2–5 \times 10^{11}$ platelets is a lifesaving procedure to prevent bleeding in patients undergoing chemotherapy or to stop bleeding in patients with a low platelet count ($<10–30 \times 10^9$ platelets/L) or with functional platelet disorders [21,15]. Each year, 300,000 PC are transfused in France (according to the French report of the General Inspectorate of Social Affairs RM2010–089 P), and over 100 million worldwide. In developed countries, altruistic donation constitutes the cornerstone of a safe and sustainable blood supply. In the absence of blood donation, no country can provide sufficient blood products to all patients requiring transfusion. Nevertheless, this system bears limitations. Blood donation requires costly testing to ensure maximum safety in terms of infection, immunity and inflammation. Furthermore, lifetime prolongation sustained by current treatments (chemotherapy, radiotherapy) results in an increased consumption of PC, in a context of stagnating donor numbers. This lack of platelets will in turn limit burgeoning clinical applications in regenerative medicine, wound healing and even cosmetics [25,13]. This anticipated shortage highlights the need to develop alternatives to blood donation best represented by scalable, on-demand bio-manufactured platelet (BMP) production, compliant with current Good Manufacturing Practices (cGMP). A number of laboratories have already initiated such developments, helped by increased knowledge in molecular and cellular mechanisms underlying platelet biogenesis and through biotechnological advances [2,11,18,22,26].

*In vivo*, MK are derived from hematopoietic stem cells (HSC) during megakaryopoiesis. This process calls for a succession of proliferation, differentiation, and maturation stages. Mature MK make then contact

*Abbreviations:* MK, megakaryocytes; PC, platelet concentrate; BMP, bio-manufactured platelet; HSC, hematopoietic stem cells; PMD, Pipette Mimetic Device; CFD, computational fluid dynamics; NP, native platelets; SA, Stress Accumulation.

* Correspondence to: UMR_S1255, EFS Grand Est, 10 rue Spielmann, F-67065 Strasbourg, France.
*E-mail address:* Catherine.strassel@efs.sante.fr (C. Strassel).

https://doi.org/10.1016/j.nbt.2023.07.002
Received 17 February 2023; Received in revised form 13 June 2023; Accepted 9 July 2023
Available online 11 July 2023

with sinusoidal vessels, where they extend cytoplasmic extensions, the proplatelets, which are subsequently detached and remodeled by blood flow to form *bona fide* blood platelets. These different steps are tightly controlled by cytokines, transcription factors and cooperating environmental cues such as cell-cell interactions, cell-matrix interactions and specific flow conditions [1,10,23]. In this optimal intricate bone marrow microenvironment, it is estimated that one MK is capable of producing 1000 to 3000 platelets [24]. BMP production aims to mimic these processes as closely as possible while ensuring maximum homogeneity, safety and stability of biological raw materials and finished products under cGMP conditions.

Several protocols have been developed, using induced pluripotent stem cells, fibroblasts, or human hematopoietic progenitors as starting cells, combining cocktails of cytokines and pharmacological agents allowing to produce proplatelet-bearing MK. However, the final stage of platelet release remained inefficient under conventional culture conditions. More recently, devices including flow regimes have improved platelet release. Most of them are scalable microfluidic reactors mimicking blood laminar flow conditions [2,11,18,22]. Despite their capacity to release functional platelets, only a low yield of 2–20 platelets/MK is obtained in these systems which need to be operated in parallel to meet large-scale production [2,18,22,17]. A leap in platelet release efficiency has been achieved by applying turbulent flow conditions to a suspension of MK. In a large culture volume (10 L) turbulent bioreactor, approximately 80 platelets/MK were generated [11]. Although shear stress and turbulent kinetic energy levels have been identified as playing a primary role in this system, the detailed release mechanisms remain to be addressed.

The present study focused on the development of a platelet release device compatible with industrial requirements. An in-depth analysis revealed that, beyond turbulence, which is now accepted as an essential parameter, the combination of new flow regime parameters could further optimize platelet release. This device relied on a bench scale platelet release method mimicking the alternating movements of pipetting cycles and was named "**P**ipette **M**imetic **D**evice" (PMD). It consists of five spherical chambers assembled in a row, each containing two calibrated cones placed in staggered positions. A correlation was established between the number of chambers, the flow rate in the device and the efficiency of platelet release. It was also validated that the released platelets were of quality, both morphologically and functionally. In order to better understand the platelet release mechanisms, a series of computational flow dynamics (CFD) analyses was performed. Local generation of unsteady periodic flows with highly turbulent regions was observed in different parts of the device. In addition, thorough analysis of MK simulation trajectories highlighted the importance of combining shear stress and its duration for efficient platelet release. This combination led to shear stress accumulation (16 Pa.s on average), a parameter not recognized so far as being important for platelet release. Overall, this study resulted in the design of a new platelet release device that is both efficient (100 BMP/MK) and compatible with industrial constraints and a better understanding of the flow regimes that govern platelet production.

## Materials and methods

### *Megakaryocyte differentiation in culture*

CD34 + hematopoietic progenitors were extracted from leukodepletion filters (TACSI, Terumo BCT, Zaventem, Belgium) and cultured for 14 days as previously described [19].

### *Biomanufactured platelet (BMP) release*

At day 14, following the addition of 0.5 μM illoprost (Ilomedine 0.1 mg/mL, Bayer AG, Wuppertal, Germany), BMP were released by 5 successive manual pipettings with a 1 mL-type cone or the newly developed device, PMD. The flow in the PMD was generated by applying a continuous vacuum (KNF, Freiburg, Germany) at the outlet. The flow rate, fixed at 80 mL/min, was measured using a miniature paddlewheel flow meter (Bio-Tech e.K, Vilshofen, Germany) placed downstream of the device or assemblies. Individual spheres were obtained by injection molding of UPS Class VI polypropylene (Saint Gobain Life Sciences, France). Assemblies were made possible by special quarter-turn locking tube assemblies equipped with EPDM seals at the inlet and outlet. Connections to tanks and other production process assemblies were made with standard weldable 2 mm diameter PVC tubes used for blood transfer (Saint Gobain Life Sciences). A single device, or assemblies, can be sterilized with gamma rays or hydrogen peroxide. The entire production configuration provided a closed system and a cGMP manufacturing process. After release, the collected BMP were centrifuged and resuspended in Tyrode's albumin buffer as previously described [5].

### *Platelet morphology and ultrastructure*

*Transmission electron microscopy*. BMP were fixed in 2.5% glutaraldehyde and embedded in Epon. Thin sections were stained with uranyl acetate and lead citrate and examined under a JEol 2100-plus microscope (Jeol, Tokyo, Japan) as previously described [5].

### *In vitro platelet studies*

*Platelet counting.* The number of released platelets was estimated using tubes containing calibration beads (BD Trucount™, BD Biosciences, San Jose, CA, USA) and antibodies to GPIIb-IIIa (Alexa-488) and GPIbα (Alexa-647). The platelet count was expressed as the number of platelets per MK present on day 7 of culture. *Platelet activation.* Platelet suspension was labeled with antibodies to GPIbα (Alexa-568) and test tubes were prepared, containing either: anti-PAC-1 antibody (Alexa-647) (anti GPIIb-IIIa in its activated form), anti-P-Selectin antibody (FITC), or the isotype control. Platelets were activated by the following agonists: thrombin 1 U/mL, CRP 10 μg/mL or a combination of CRP 10 μg/mL and TRAP-6 50 μM during 10 min at 37 °C. The percentage of activated platelets was analyzed by flow cytometry. *Glycoprotein expression assays*. The platelet suspension was separated and labeled with antibodies directed against GPIIb-IIIa (Alexa-488), GPIbβ (Alexa-568), GPV (Alexa-647), GPIX (Alexa-568) and CD9-PE. After incubation for 30 min at room temperature, samples were analyzed by flow cytometry. FMOs (Fluorescence Minus One) were performed to determine the analysis windows when using multiple fluorochromes. Cytometric analyses were performed using Fortessa X20 (Becton Dickinson, Franklin Lakes, NJ, USA).

### *In vivo functionality*

*BMP recirculation after transfusion.* Experiments were performed according to a recent publication [5]. In brief, following their release, platelets were resuspended in a preservation solution consisting of one third plasma and two thirds Intersol (Fresenius Kabi, Homburg, Germany) at a concentration of $5 \times 10^5$ platelets/μL. Then, $5 \times 10^7$ BMP or native human platelets from CP transfusion bags were injected through the retro-orbital vein into NSG mice (NOD.Cg-Prkdc scid, Il2rg tm1Wjl/SzJ) previously depleted of macrophages by injection of clodronate liposomes at day -1. Whole blood samples were drawn before and at different time points after transfusion and the proportion of circulating BMP or native platelets (NP) recorded in the acquisition gate 3 min after transfusion was arbitrarily set to 1.

### *Flow simulations in mathematical models*

In a preliminary stage, flow conditions inside the cone and the test tube during aspiration or discharge were inferred from simplified flow

simulations using the Flow Simulation tool embedded in Solidworks 2020 CAD software. A detailed geometric model of the tube and cone assembly was first generated in Solidworks. This geometry is automatically meshed in the simulation tool and standard wall laws are applied depending on the mesh refinement. Secondly, steady continuous flow conditions were applied between the tube and cone top openings in order to generate either a continuous aspiration or a continuous discharge. Once the computation converged, streamlines were generated, and animations thereof were recorded for further analysis. The same procedure and tools were used to outline the generic features of the final release device.

After development of the new design, detailed flow conditions inside the release device were determined by computational fluid dynamics (CFD) simulations using Fluent 2020R2 finite volume software package (ANSYS Inc., Canonsburg, PA, USA). The simulations were performed in two consecutive steps. The first one consisted of a simple transient viscous laminar simulation with periodic flow conditions between the inlet and outlet of a single chamber geometry. The boundary conditions were set in terms of pressure gradient similar to the one derived from previous assessments of platelet production under different flow rates. This process resulted in a hybrid mesh with a total of 5322,000 elements – 5964,000 nodes. The results were used to initiate the second step consisting of a steady turbulent flow simulation. For this purpose, a k-omega transition SST (4 equations) model was implemented using the same mesh and boundary conditions (Supplemental Data) [14]. Quality and accuracy of the solution were monitored through a mesh sensitivity test. The numerical simulations of the flow gave access to pressure and velocity at any position/location of the computational domain and these values were used to define the local gradient of the velocity tensor and other physical quantities of interest. To assess the dynamic of BMP and cells within the flow, we performed numerical simulations of their trajectories. For this purpose, trajectories of small inert spherical particles dragged into the flow were inferred by a Lagrangian 3D unsteady model based on the achieved CFD simulations. According to the low number and size of platelets, non-reciprocal actions of particles on the flow was assumed and therefore a one-way coupling was implemented. For each particle size under consideration, 2, 5 or 10 μm, a set of 1000 trajectories was computed from particles seeded randomly in the inlet section and the particle histories data through the single chamber were statistically analyzed. Accumulation effects over multiple chambers were deduced from those observed in this single chamber by simple addition.

### *Ethics statement*

Human studies were performed according to Helsinki declaration. Control human samples were obtained from volunteer blood donors who gave written informed consent recruited by the blood transfusion center where the research was performed (Etablissement Français du Sang-Grand Est). All procedures were registered and approved by the French Ministry of Higher Education and Research and registered under the number AC_2015_2371. The donors gave their approval in the CODHECO number AC_2008_562 consent form, in order for the samples to be used for research purposes. NSG mice were housed under pathogen-free conditions and all procedures were performed in accordance with the European Union Guideline 2010/63/EU. The study was approved by the Regional Ethical Committee for Animal Experimentation of Strasbourg, CREMEAS (CEEA 35) and registered under the number 10669.

### *Statistical analyses*

Results were expressed as the mean ± SEM and statistical comparisons were performed using an unpaired, two-tailed Student's t-test or one-way ANOVA followed by the Bonferoni post-hoc test (Prism, GraphPad Software Inc., San Diego, CA, USA). P values of less than 0.05 were considered to be statistically significant ($P > 0.5$ [ns.]; $P < 0.04$ [*]; $P < 0.004$ [**]; $P < 0.001$ [***]; $P < 0.0001$ [****]).

## Results

### *Manual pipetting procedure at the origin of the platelet release device*

Platelet release from proplatelet-bearing MK requires the generation of appropriate flow regimes. As previously published, pipetting (aspiration and discharge through a 1 mL cone) represents an empirical but efficient method for the release of BMP. Here, following a gradual increase in the number of pipetting cycles, a maximum of 119.48 ± 25.17 BMP/MK was obtained after 5 pipetting cycles, corresponding to a 3.8-fold increase compared to only 1 pipetting (119.48 ± 25.17 vs. 31.23 ± 7.62 BMP/MK, 5 vs. 1 pipetting respectively) (Fig. 1A). Interestingly, we observed that only continuous pipetting allowed optimal platelet release compared to pauses between each pipetting cycle (R1, R2…) (Fig. 1Bi) or each aspiration or discharge (PR1, PR2…) (Fig. 1Bii). These results indicated the importance of applying a periodic hydrodynamic load at frequency of 0.7 Hz (f=1/T; one cycle of aspiration discharge=1.42 s) on proplatelet-bearing MK to promote their release and subsequent remodeling into platelets. Of note, all the BMP produced were functional regardless of the number of pipetting cycles, as witnessed by GPIIb-IIIa activation detected by PAC-1 binding following thrombin activation (Fig. 1C). This manual method is therefore efficient to produce functional BMP but is not amenable to large scale nor cGMP compliant. For this purpose, a " pipette-mimetic " platelet release device was designed after a preliminary design stage during which Computational Fluid Dynamics (CFD) simulations of either aspiration or discharge were analyzed.

### *Design of the "Pipette-mimetic device" (PMD)*

CFD simulation of the discharge revealed a significant acceleration of fluid velocity as the cone narrowed, with a hot spot (in light blue and green) at the apex of the cone, followed by a deceleration and subsequent recirculation of the fluid in the tube. A reverse behavior was observed following fluid aspiration (Suppl. Video 1). Based on this analysis, we designed a device with specified sizes and dimensions as detailed in Fig. 2A. In brief, two calibrated 1 mL capacity-pipetting cones were placed in a sphere to favor fluid recirculation. They were arranged in a staggered configuration to mimic the discharge phase (inlet) while the passage through the second cone reproduced the aspiration phase (outlet) (Fig. 2A). The cell suspension was aspirated through the device by applying a negative pressure, at a flow rate of 80 mL/min (based on pipetting measurements, data not shown). Subsequently, to ensure that the design of the platelet release device mimicked the flow instability and periodic hydrodynamic loading observed during pipetting cycles, we simulated the behavior of the particles in a sphere. As previously observed during the pipetting cycles, we confirmed an acceleration of the fluid at the apex of the discharge and aspiration cones and a fluid recirculation into the sphere (blue gradient) (Suppl. Video 2). To manufacture the platelet release device in its definitive design, we evaluated the optimal number of spheres for maximal BMP release. Interestingly, a succession of 5 spheres was determined to be optimal (92.52 ± 8.90 BMP/MK), matching the number of cycles in the manual procedure (Fig. 2B). Overall, these results validated the device as a Pipette Mimetic platelet release Device: PMD. This device has the advantage of processing 80 mL of MK suspension per minute with a yield of approximately 100 PMD-released BMP/MK. It allows us to meet the requirements of large-scale platelet production. Moreover, its compact design (5 ×5×15 cm) allows it to be easily integrated to the culture processes under a laminar flow hood (Fig. 2C).

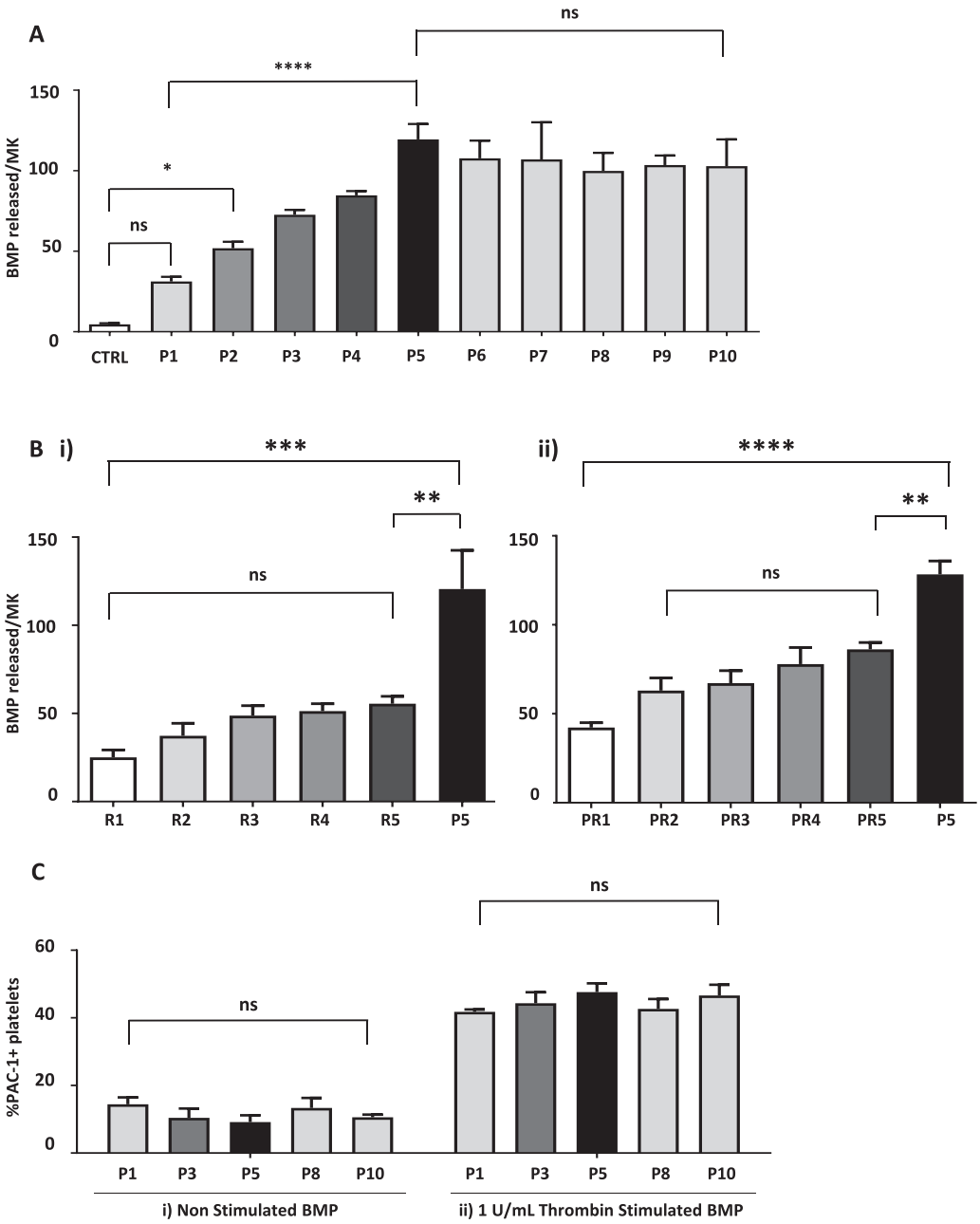


**Fig. 1.** Manual pipetting as a platelet release process. A) Bar graph representing the yield of platelets (BMP)/MK seeded at day 7 according to the number of pipetting cycles (119.48 ± 25.17 vs. 31.23 ± 7.62 BMP/MK, 5 vs. 1 pipetting respectively; n = 6). Bi) Bar graph of the number of BMP/MK released with different numbers of pipetting compared to a rest time between each aspiration and each discharge (R1 to R5), compared to 5 classical continuous pipetting of aspirations and discharges without rest time (P5) (55.52 ± 4.21 BMP/MK vs 120.60 ± 21.96 BMP/MK, R5 vs P5, n = 4). Bii) Bar graph of the number of BMP/MK released with a rest time between each complete pipetting movement (aspiration + discharge) (PR1 to PR5), compared to 5 continuous pipettings (P5) (86.22 ± 3.79 BMP/MK vs 128.3 ± 7.5 BMP/MK, PR5 vs P5, n = 3). **C)** Activation of BMP. Non stimulated (left panel) and stimulated (right panel). An increase in PAC-1 antibody binding is observed in thrombin treated BMP, regardless of the number of pipetting cycles, as compared with resting controls (41.76 ± 0.69, 44.33 ± 3.23, 47.63 ± 2.57, 42.66 ± 2.91, 46.63 ± 3.17; 1, 3, 5, 8 and 10 pipettings respectively for stimulated BMP; n = 3).

*Morphological and functional characterization/assessment of PMD-released platelets*

To validate the performance of this new platelet release device, we analyzed the quality of the platelet release. A transmission electron micrography (TEM) analysis demonstrated that PMD-derived platelets were ultrastructurally identical to human donor platelets. Indeed, they displayed a microtubule marginal band, a key feature of native platelets (NP). In addition, they were anucleate and possessed organelles, including mitochondria, open canalicular systems (OCS) and granules (α and δ). However, they presented an ovoid rather than flat shape and their diameter was enlarged by 2.27-fold as compared to the bulk of NP (2.46 ± 0.55 µm vs 5.60 ± 0.5 µm, NP vs. PMD-released BMP, respectively) having a similar nature as newly generated platelets, which are known to be enlarged (Fig. 3A). The PMD-released BMP quality was documented firstly by the presence of more than 90% of the main GP at the platelet surface (Fig. 3B). Secondly, their activation potential was demonstrated by their capacity to bind PAC-1 and to externalize P-Selectin (P-Sel). As previously reported, PMD-released BMP exhibited a slight pre-activation without preventing them from responding to different agonists. Indeed, even if PMD-released BMP appeared to be less activated in response to thrombin (88.1 ± 2.3 vs 52.4 ± 2.5% PAC1 + and P-sel positive platelets, NP vs. PMD-released BMP, respectively), they showed similar PAC-1 and P-Sel activation responses to CRP or to a TRAP-6 +CRP combination (33.7 ± 9.2 vs 29.5 ± 2.6% PAC1 and P-sel positive platelets, NP vs. PMD-released BMP, respectively for CRP activation and 52.8 ± 6.5 vs 51.2 ± 1.8% PAC1 and P-sel positive platelets, NP vs. PMD-released BMP, respectively for a combination of CRP and TRAP-6 for activation) (Fig. 3C). Importantly, $5 \times 10^7$ PMD-released BMP recirculated with good efficiency following transfusion with a transient increase between 15 and 240 min of recirculation. Following a plateau, they were removed at the same pace as NP. Therefore, PMD-released BMP were able to recirculate and even exhibited a longer half-life (4.33-fold) than platelets derived from platelet concentrates

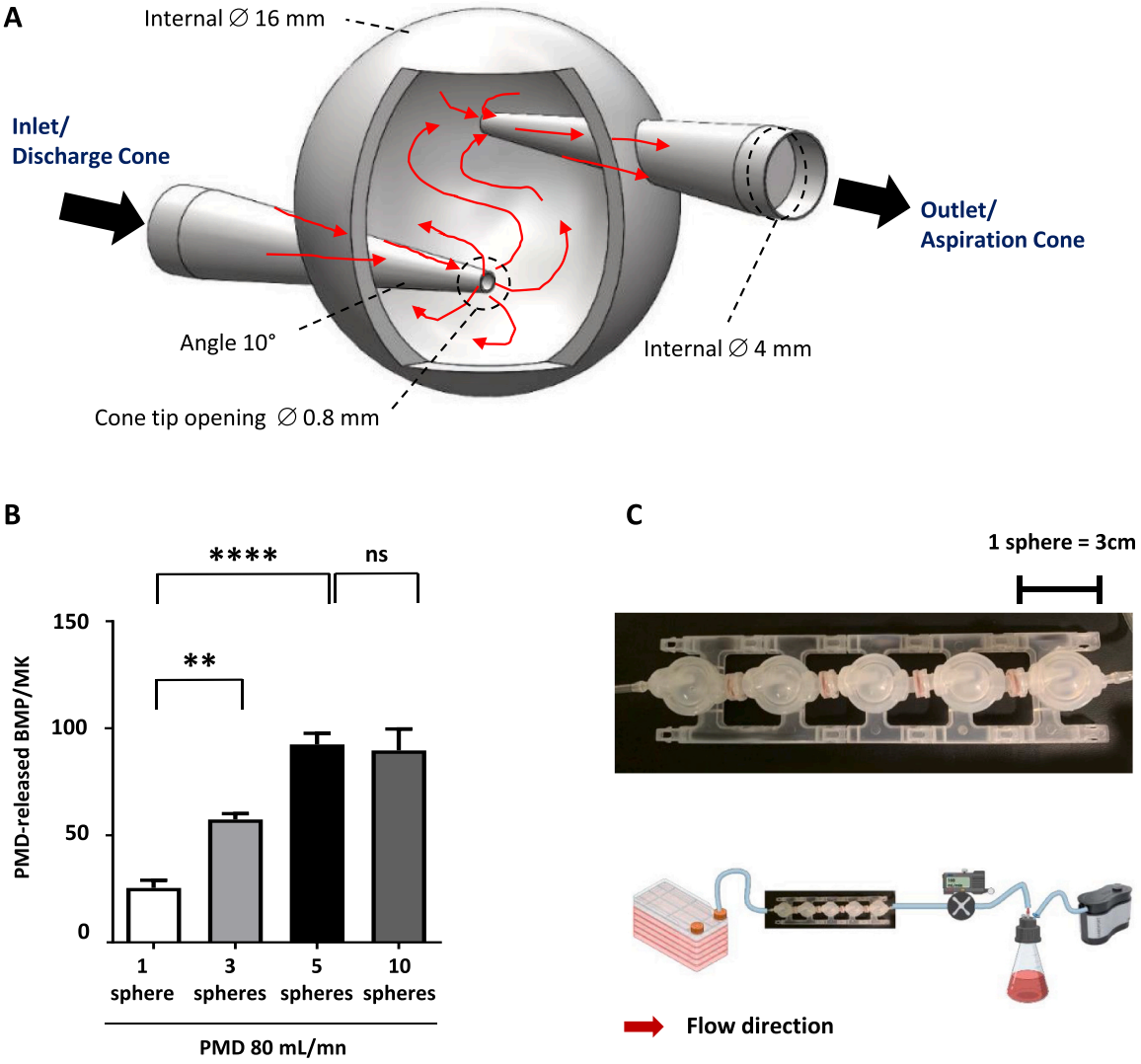


**Fig. 2.** Platelet release device design and performance. A) Internal view of a PMD sphere with cone positioning and dimensions. It also presents a schematic view of flow motions (red arrows) within one PMD block. Black arrows indicate direction of the flow and thus the inlet and outlet cones. B) Bar graph representing the yield of BMP/MK according to the number of PMD spheres (25.43 ± 3.62, 57.40 ± 2.76, 92.52 ± 5.14, 89.64 ± 10.02 PMD-released BMP/MK; 1, 3, 5 spheres respectively; n = 3). C) Sketch of the PMD in its final form in operation in a closed circuit.

(17 h vs 4 h, PMD-released BMP vs. NP, respectively) (Fig. 3D). Overall, these data provided support for the morphological and functional qualities of PMD-released BMP.

*Characterization of flow regimes in the PMD*

To better understand the parameters governing the performance of the device on platelet release, we carried out an in-depth characterization of flow regimes. Firstly, we performed an analysis of the behavior of the flow rate as a function of the pressure drop between the inlet and outlet sections of the device. The linear behavior demonstrated the laminar nature of the bulk flow (Fig. 4A). To better characterize the flow features in different regions of the PMD we next performed a detailed analysis of the CFD data (Fig. 4B). At a flow rate of 80 mL/min, different velocity magnitude profiles were observed along the inlet and outlet cone axes (Fig. 4C). In the discharge cone, as the cone narrowed, the velocity increased from ~0.1 to ~3.5 m/s, corresponding to an average acceleration of ~490 m/s$^2$ in the cone (section a1, j1). Then, the velocity remained constant for a short distance and dropped to 0 at the chamber wall at position r1 (Fig. 4Ci) generating a strong recirculation in the spherical chamber. Concomitantly, upon entering the aspiration cone, an increase in velocity was observed from 0 at the chamber wall to ~4.5 m/s shortly after the cone tip, corresponding to a drastic acceleration (section a2). In the cone, the velocity slowly declined to ~0.1 m/s in the wide section (section j2) with an average deceleration of ~800 m/s$^2$ (Fig. 4Cii). Such successions of accelerations and decelerations are likely to destabilize the flow and lead to a turbulent flow. As can be inferred from the turbulence intensity scale (Suppl. Data) [14,8,3,6,4,7], high turbulence intensity was encountered at the acceleration zones, while an average turbulence intensity of 5% was observed in the wide section of the discharge and aspiration cones (Suppl. Fig. 1). Such tendencies are confirmed by variations of the local Reynolds number which are about 2400 and 3000 in the $Z_1$ and $Z_2$ sections, respectively.

*Particles trajectories history influence their residence time in PMD*

The residence time ($t_{res}$) of 1000 particles of different sizes, from 2 to 10 μm, was analyzed by computational flow simulations by setting the flow rate at 80 mL/min. While all particle trajectories were subjected to the same flow conditions, as defined previously: acceleration (j1, j2), deceleration, recirculation (r1, r2), not all the particles followed the same trajectories (Fig. 5A). Indeed, while at the turbulent zone of the

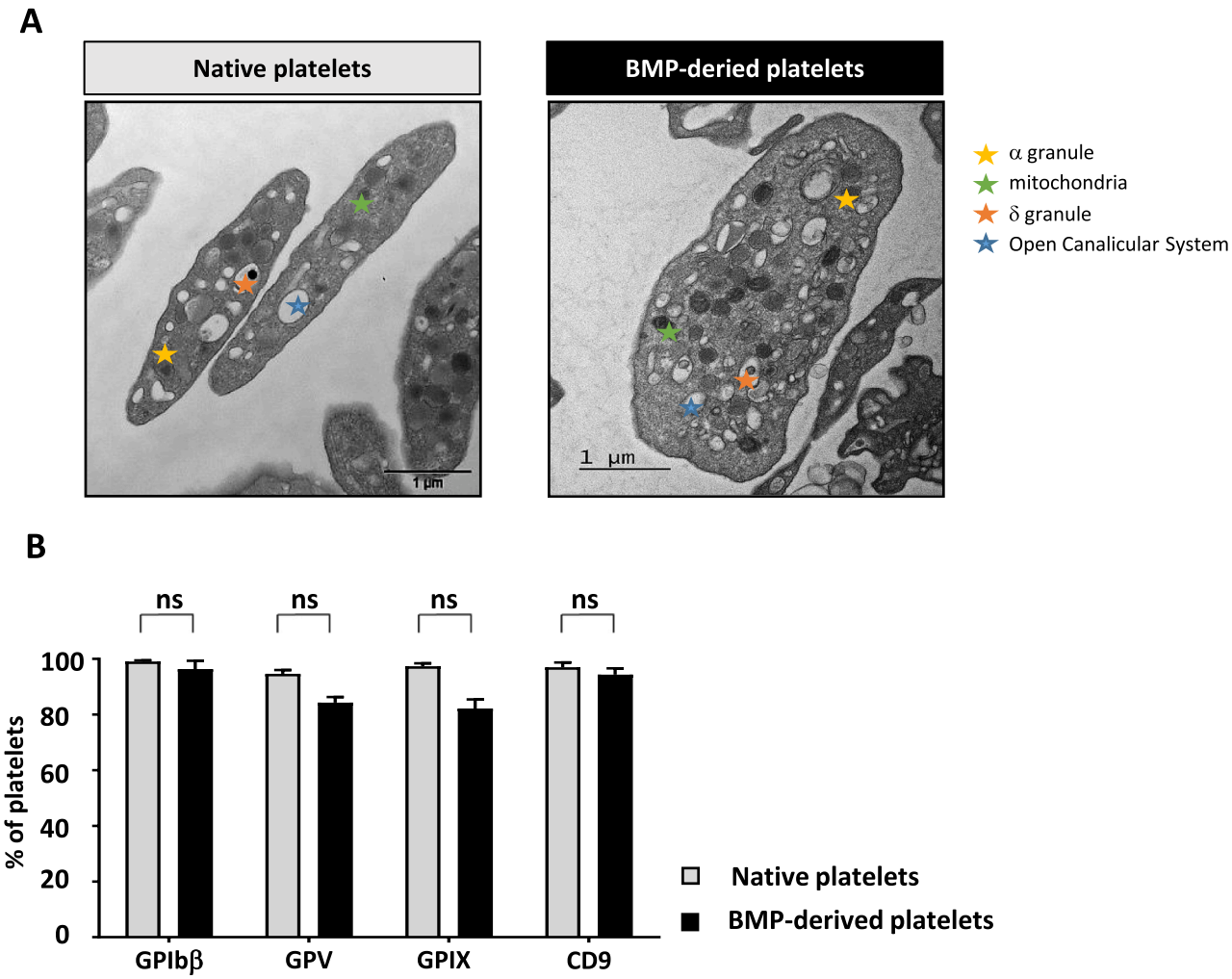


**Fig. 3.** Morphology and function of PMD-released BMP. A) Representative transmission electron microscopy (TEM) images of NP (left panel, Bar = 1 µm) and PMD-released BMP (right panel, Bar = 1 µm). Figure legend is annotated on the image. B) The bar graphs represent the percentage of platelets (NP and PMD-released BMP) expressing major surface glycoproteins, n = 4. C) *In vitro* functionality of PMD-released BMP. PAC-1 binding and Pselectin activation of washed NP and PMD-released BMP without stimulation (0.5 ± 0.4 vs 9.2 ± 2.7% PAC-1 and Psel positive platelets (NP vs PMD-released BMP); n = 3 and n = 4), or stimulated with thrombin 1 U/mL (88.1 ± 2.3 vs 52.4 ± 2.5% PAC-1 and Psel positive platelets (NP vs PMD-released BMP); n = 3 and 4), or stimulated with CRP 10 µg/mL (33.7 ± 9.1 vs 29.5 ± 2.6% PAC-1 and Psel positive platelets (NP vs PMD-released BMP); n = 3 and 4), or stimulated with a combination of CRP 10 µg/mL and TRAP-6 50 µM (52.8 ± 6.5 vs 51.2 ± 1.8% PAC-1 and Psel positive platelets (NP vs PMD-released BMP); n = 3 and 4) D) Platelet recirculation mouse model. Human platelets were detected and counted by flow cytometry. NP count decreased linearly over time whereas PMD-released BMP count reached a maximum 1 h after injection and then progressively decreased. Mean of 3 independent experiments. PMD-released BMP exhibit a longer half-life (4.33-fold) than native platelets (17 h vs 4 h, PMD-released BMP vs. NP respectively); n = 3.

discharge (j1), all the particles followed the same path, after the deceleration (r1), several particles moved over a short distance, whereas others recirculated several times into the sphere, before being re-accelerated and unilaterally aspirated through the turbulent region (j2). At the exit of the aspiration cone, whereas most particles went through the next sphere, some of them were drawn back into a recirculation (r2). These differences in particle behavior led to different path lengths, which in turn affected their $t_{res}$. The average value of $t_{res}$ was about 1.6 s, ranging from 0.26 to 9.9 s (Fig. 5B) and decreased linearly with increasing flow rate (Fig. 5C). We also showed that shifting the size of the particles from 2 to 10 µm had a negligible influence on the linear dependency of $t_{res}$ towards flow rate (Suppl. Fig. 2).

*Shear stress accumulation analysis*

$t_{res}$ variations coupled to the exposure of cells to different flow characteristics resulted in different hydrodynamic loading of each particle, objectified by the scalar shear stress (SS). Since there is a variety of trajectories, the SS was described by a non-unique statistical description. The variation of the scalar shear stress as a function of flow rate was generated from mean values of SS from the 1000 simulated trajectories. The analysis of the mean SS showed a linear increase with flow, and detailed analysis followed by the decomposition of the local hydrodynamic shear stress components into viscous and turbulent contributions showed that the turbulent shear stress fully dominated the SS history (Fig. 6A). Indeed, when analyzing the shear stress values at a flow rate of 80 mL/min, the total shear stress reaches a value of 115 Pa, while the average viscous shear stress contribution is only about 7.5 Pa.

Most of the cells have been shown to be sensitive to both shear stress and loading duration, which can be analyzed through scalar shear Stress Accumulation (SA) computations (Suppl. Data) [8,3,6,4,7]. Whereas SA statistics were influenced by the various trajectories of particles (data not shown), we demonstrated a linear increase in the average value of SA until the optimal 80 mL/min flow rate, where SA reaches a value of

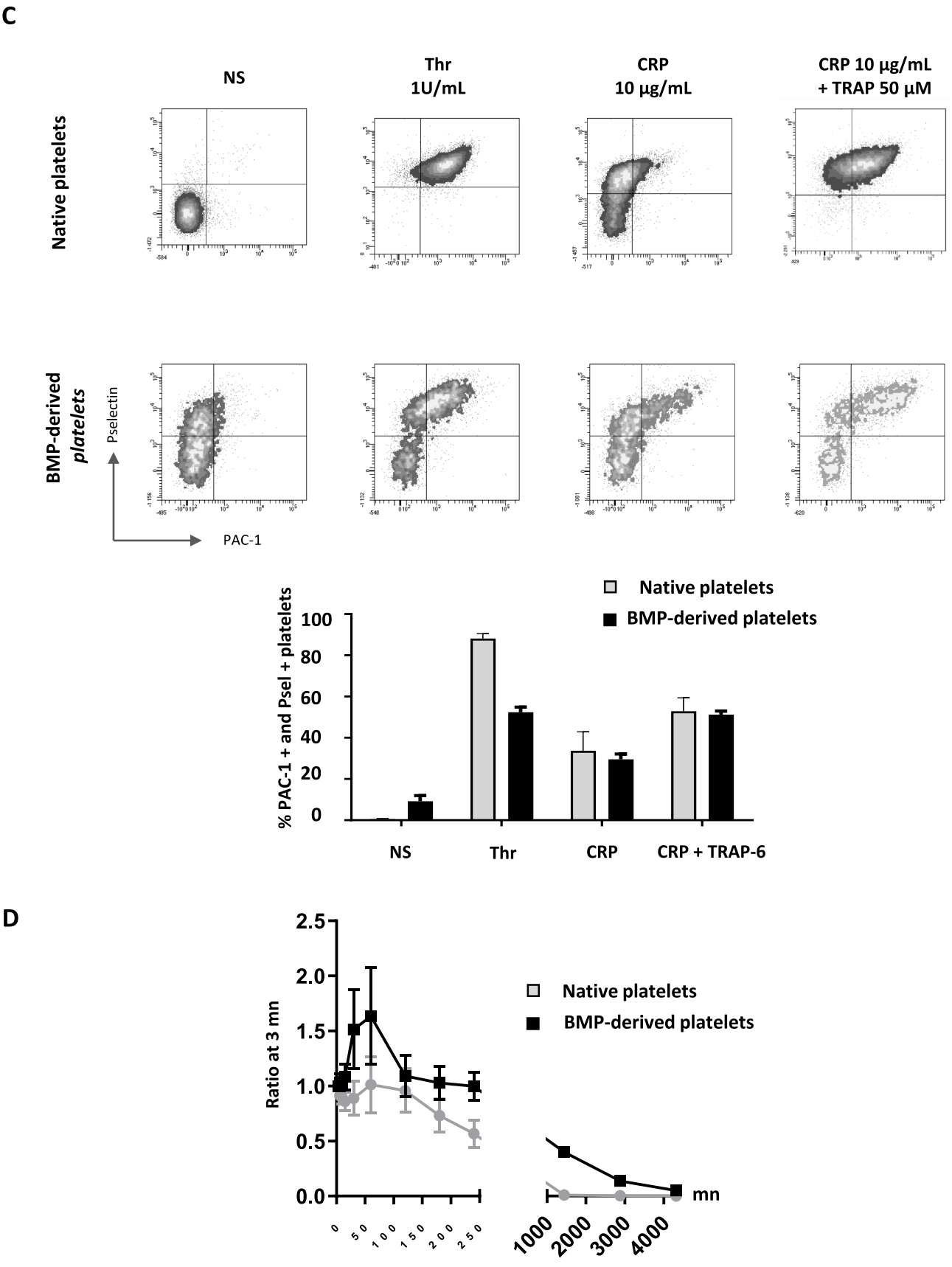


**Fig. 3.** (*continued*).

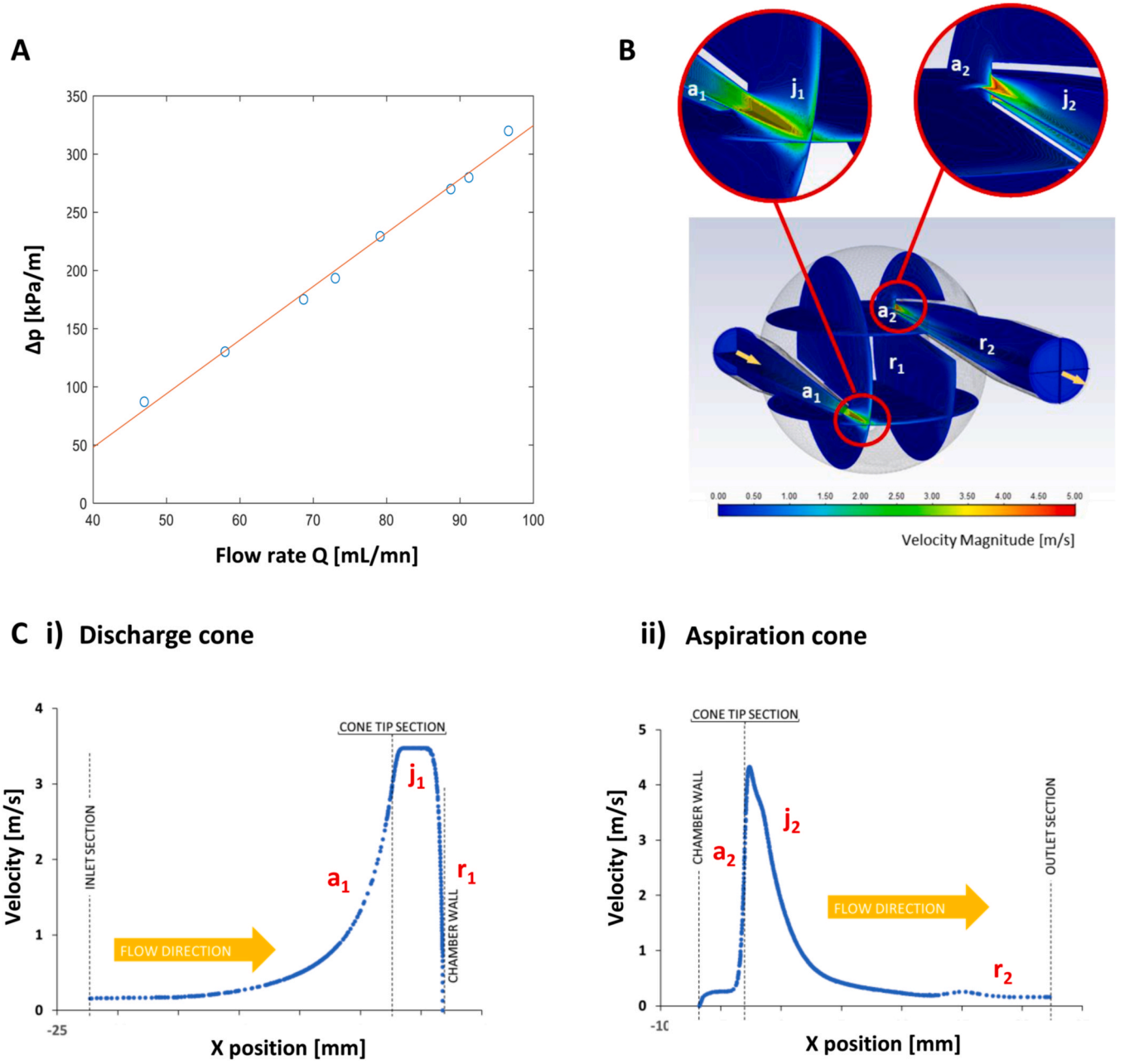


**Fig. 4.** Characterization of flow regimes within the PMD. A) Relationship between inlet/outlet pressure drop in the PMD (kPa/m) and flow rate Q (mL/min). The linear relationship highlights an overall laminar flow regime. B) CFD-computed velocity field. Color contours show the variations in velocity. C) Velocity magnitude along the longitudinal axis of i) discharge (left) and ii) aspiration (right) cones. Acceleration is observed in the area of cone tips (a1 and a2).

16 Pa.s in the single simulated PMD chamber (Fig. 6Bi). CFD visualization of the chamber was carried out at the same flow rate to observe the scalar shear stress distribution (Fig. 6Bii). As before, different profiles were observed along the axes of the inlet and outlet cones. These sections correspond to the regions of interest described above, i.e., colocalized with high turbulence intensity regions (sections $Z_1$ and $Z_2$).

Beyond 80 mL/min, the SA decreased, accompanied by a decrease in PMD-released BMP as observed at a flow rate of 90 mL/min (Fig. 6C). Altogether, these results showed that, in addition to turbulence, other parameters influence the rupture of proplatelets into platelets such as the residence time of the cells in the device and the scalar shear stress accumulation. These new parameters should be taken into account in order to optimize platelet release devices.

## Discussion

This work has led to the development of an efficient platelet production device easily implemented in any type of bioreactor for clinical grade platelet production. In addition, this device provided an interesting groundwork to study the flow parameters favoring platelet release. Indeed, this allowed to identify, along with turbulence, periodic hydrodynamic loading and shear stress accumulation as two key parameters for platelet release, providing important information for the optimization of current and future platelet release devices.

Following a detailed analysis of the effects of flow constraints during manual pipetting, an automatic and cGMP compliant platelet release device called PMD for “Pipette Mimetic Device” was engineered. With a high yield of 100 PMD-released BMP/MK and a flow rate of 80 mL/min, this device allows for large-scale platelet production while preserving

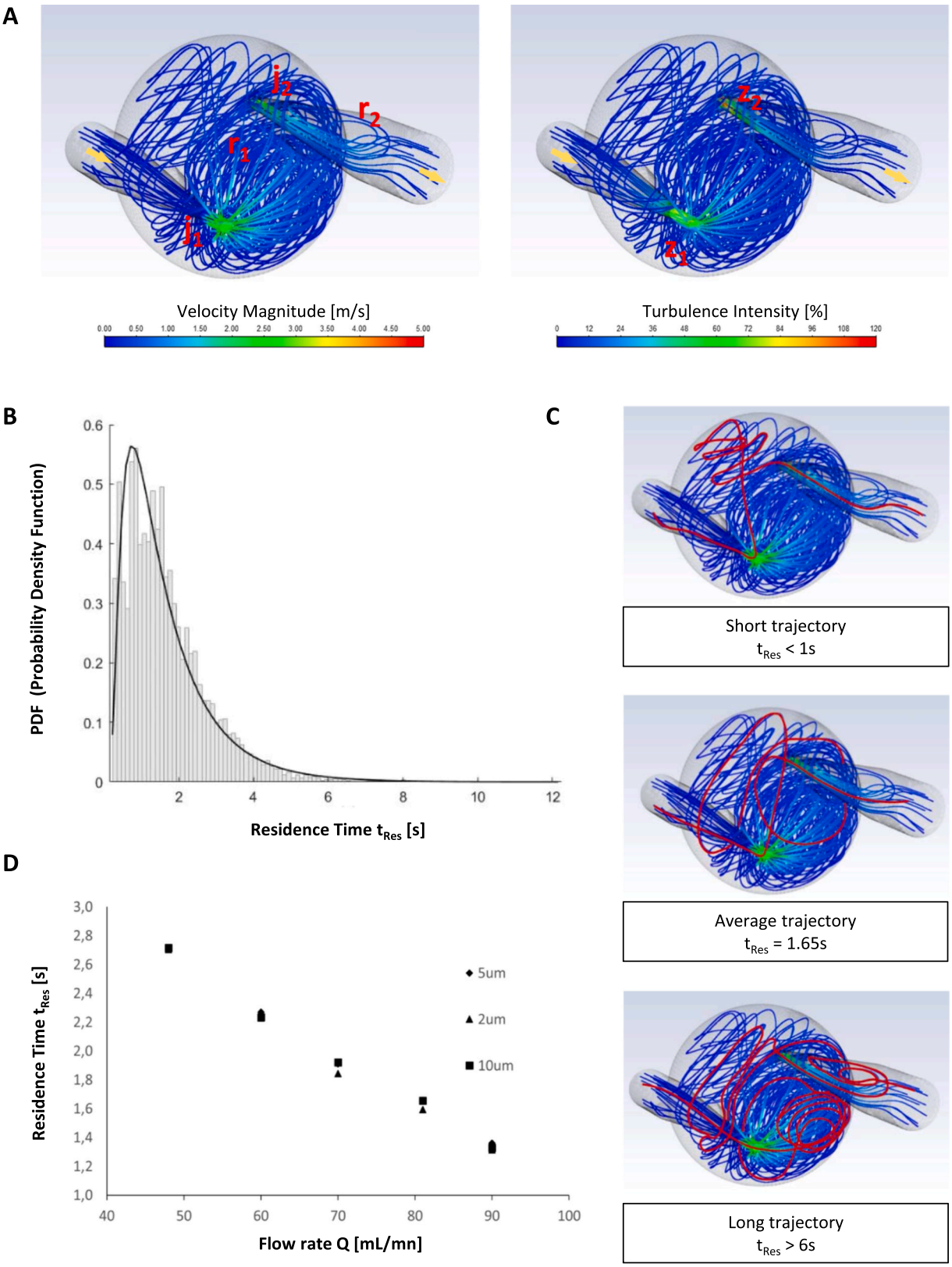


**Fig. 5.** Particle trajectories influenced by flow features, velocity gradients and turbulence intensity. A) Particle trajectories as determined by the Particle Tracing Module. Simulations of 10 particles trajectories of different sizes. The fastest particles matched the high velocity and high turbulence regions of the PMD. B) Measurements of particles resident time with a flow rate of 80 mL/min. The bar graph represents the proportion of particles (PDF = Probability Density Function) as a function of residence time. Solid line represents the best fit over the data (Birnbaum Saunders distribution). C) Examples of the different trajectories followed by the particles inside a sphere. Complex trajectories imply long residence times. The mean resident time is less than 2 s D) The graph represents the average residence time as a function of the applied flow rate and for different particle sizes. Whatever the particle size, as the flow rate increases, the residence time decreases.

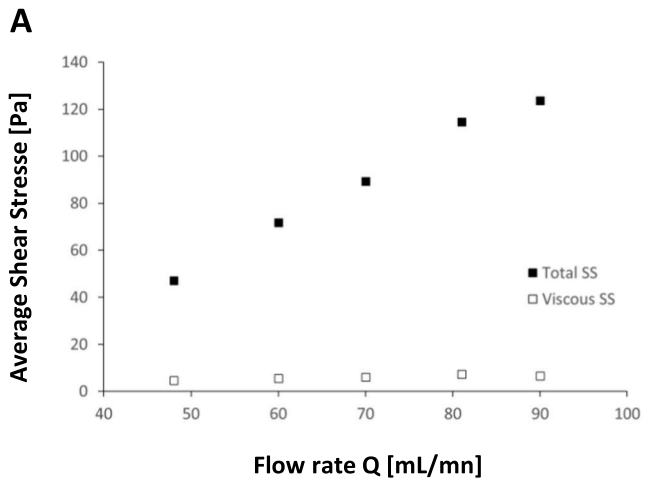


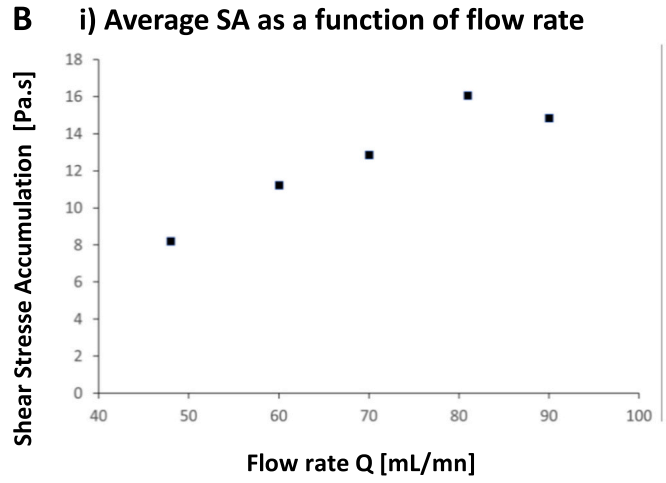


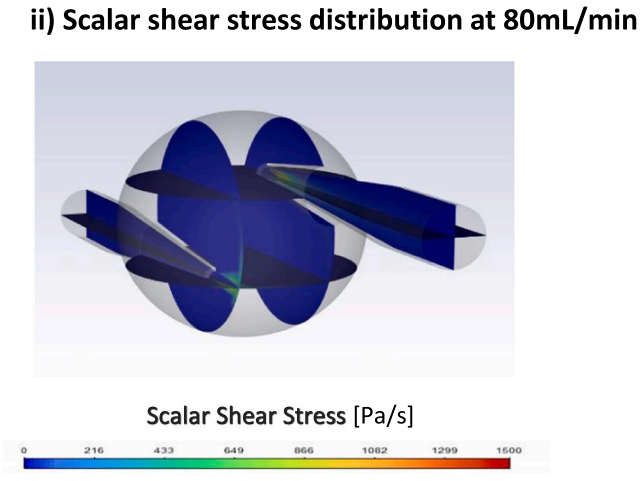


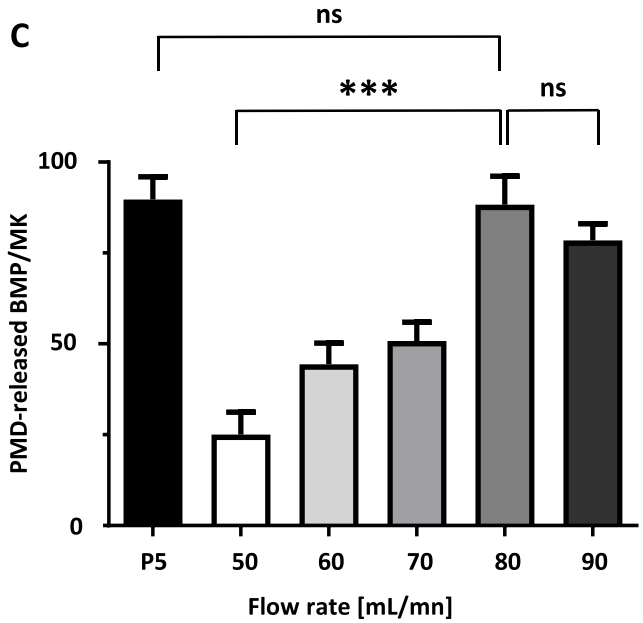


**Fig. 6.** Shear Stress Accumulation as a new parameter for an efficient platelet release. A) Dot plot of the Average Shear Stress (SA) intensity as function of flow rate, showing the decomposition of the local hydrodynamic shear stress components into viscous (white squares for Viscous SS) and turbulent contributions (black squares for Total SS (viscous +turbulent)). B) i) Dot plot representing the mean value of Shear Stress Accumulation (SA) according to the flow rate and ii) CFD analysis of the scalar shear stress distribution. Color contours show the variations of intensity at a flow rate of 80 mL/min. C) Bar graph of PMD-released BMP as function of flow rate.

their quality. Despite their larger size and signs of slight pre-activation, which has been classically observed in other studies [11,16], they were capable of responding to in vitro stimulation and to recirculate after transfusion, even longer than NP (4.33-fold) (Fig. 3). This accelerated elimination of NP compared to PMD-released BMP platelets from the circulation would appear to be related to the changes that accumulate on the platelet surface over time. Indeed, with age, platelets mainly increase the phosphatidylserine and the deglycosylation of membrane glycoproteins, which either increase the availability of clearance ligands or eliminate anti-clearance signals [12,9]. Thus, NP exhibiting an age continuum from young to old are gradually eliminated. In contrast, BMP-derived platelets are produced synchronously and display the features of young platelets upon transfusion, as evidenced by the large amounts of RNA they contain (data not shown). Therefore, with fewer surface protein modifications, PMD-released BMP elimination would be delayed, and their recirculation half-life would be longer. The yield of 100 PMD-released BMP is quite substantial for in vitro conditions, but is still far from the yields reached in vivo (1000–3000 platelets/MK) [24]. This low yield does not disprove the effectiveness of the device, but rather signs the current inability to produce fully mature MK, since confocal analysis of the MK following their passage through the device revealed only a thin ring of cytoplasm around the MK nucleus (Suppl. Fig. 3A). These results demonstrated that the continuous passage of proplatelet-bearing MK in the device where they were subjected to periodic but calibrated acceleration and deceleration of flow was indeed sufficient to exhaust the membrane and favor optimal platelet release.

Importantly, the PMD offers several competitive advantages for industrial cultured platelet production. Despite being manufactured under cGMP requirements, production cost was very low due to our capacity to design the mold to produce the device. In addition, platelet release at a flow rate of 80 mL/min, occurs fast, and since the device is compact, it can be easily implemented into the workflow of any cell culture system. For example, releasing $10^{11}$ platelets from a 10 L culture containing $10^{9}$ MK would take 125 min with a single device, and only take 30 min with four PMDs mounted in parallel at the outlet of the bioreactor. Of note, this shorter time is consistent with the half-life of prostacyclin, which must be added to significantly limit the risk of excessive platelet pre-activation during platelet release.

From a mechanical standpoint, a detailed characterization was acheived of the flow parameters that promote platelet release in the PMD. In addition to hot spots of turbulences, it was revealed that application of a periodic hydrodynamic loading at an adequate frequency on the proplatelet-bearing MK is required to support the optimal release of platelets (Fig. 1B). The observation that more than 5 spheres did not lead to a higher platelet release suggested that the optimal periodic hydrodynamic load had been achieved to drive the optimal rupture of proplatelets-bearing MK and promote their cytoskeletal remodeling to subsequently form high grade platelets. Finally, the existence was also highlighted of a parameter that accounts for an equilibrium between the intensity of the applied forces and the residence time of the cells in the device, i.e., the shear stress accumulation (SA) (Fig. 5). These observations must be considered with respect to the knowledge accumulated from studies carried out on bubble fragmentation in turbulent flow fields of suspended media, where the authors showed that these phenomena depended not only on the level of stress encountered by the bubbles, but also on a time scale [20]. Indeed, this work emphasized that fragmentation could not be quantified by the stress criteria alone, but that the competition between different time scales was just as important, since instead of being slowly and durably elongated by flows at their own scales, bubbles are fragmented in turbulence by small eddies via an intense local deformation burst and in a short period of time. In view of this study, and given that the PMD exhibits turbulent fluctuations in mechanical quantities over a wide spatial and temporal spectrum, the periodic turbulent flow generated could also lead, in a similar way to bubble fragmentation, to the fragmentation of mature MK into small platelets under the control of the mechanical strength of the cell membrane (cytoplasmic membrane and demarcation membrane system) and the characteristics of the local flow.

Although not reported until now, these parameters, SA and optimal periodic hydrodynamic loading, were already present in the latest devices developed. Indeed, to promote efficient platelet release, the bioreactor developed by K. Eto required up and down movement (350 mm/s) for 3 days and Zhao et al.'s bioreactor required 18 passages of MK through the lung [11,26].

## Conclusion

To conclude, this device offers many advantages: cGMP compliance, low production cost and a process of 80 mL of media per minute. All these advantages make the PMD an easy-to-use and inexpensive platelet release device that can be easily implemented in any bioreactor. In addition, this study also highlighted two new universal parameters that appear crucial for optimal platelet release from MK, periodic hydrodynamic load and sufficient shear stress accumulation.

## CRediT authorship contribution statement

C.S., A.P., L.M. and Y.K conceived and designed the experiments; A.P and L.M. performed the in vivo and in vitro experiments; A.E. performed electron microscopy; Y.K. and O.B. performed computational fluid dynamics simulations and all associated calculations; A.P., L.M. and C.S analyzed the data; C.S., A.P., L.M., Y.K., C.G., and F.L. discussed the techniques and results; C.S., C.G and F.L. supervised the work; and A.P., C.S., Y.K. and L.M wrote the paper.

## Declaration of Competing Interest

The authors declare no competing financial interests.

## Data availability

Data will be made available on request.

## Acknowledgements

The authors thank M.Freund for managing animal facility at UMR_S1255.

This work was supported by funds from the Association Nationale de la Recherche et de la Technologie (ANRT to A. Pongerard, PhD candidate).

## Appendix A. Supporting information

Supplementary data associated with this article can be found in the online version at doi:10.1016/j.nbt.2023.07.002.

## References

[1] Becker RP, De Bruyn PPH. The transmural passage of blood cells into myeloid sinusoids and the entry of platelets into the sinusoidal circulation; a scanning electron microscopic investigation. Am J Anat 1976;145(2):183–205. https://doi.org/10.1002/aja.1001450204.

[2] Blin A, Le Goff A, Magniez A, Poirault-Chassac S, Teste B, Sicot G, et al. Microfluidic model of the platelet-generating organ: beyond bone marrow biomimetics. Sci Rep 2016;6(1):21700. https://doi.org/10.1038/srep21700.

[3] Bludszuweit C. Model for a general mechanical blood damage prediction. Artif Organs 1995;19(7):583–9. https://doi.org/10.1111/j.1525-1594.1995.tb02385.x.

[4] Chan CHH, Simmonds MJ, Fraser KH, Igarashi K, Ki KK, Murashige T, et al. Discrete responses of erythrocytes, platelets, and von Willebrand factor to shear. J Biomech 2022;130:110898. https://doi.org/10.1016/j.jbiomech.2021.110898.

[5] Do Sacramento V, Mallo L, Freund M, Eckly A, Hechler B, Mangin P, et al. Functional properties of human platelets derived in vitro from CD34+ cells. Sci Rep 2020;10(1):914. https://doi.org/10.1038/s41598-020-57754-9.

[6] Faghih MM, Sharp MK. Modeling and prediction of flow-induced hemolysis: a review. Biomech Model Mechanobiol 2019;18(4):845–81. https://doi.org/10.1007/s10237-019-01137-1.

[7] Fang J, Sun X, Liu S, Yang P, Lin J, Feng J, et al. Shear stress accumulation enhances von willebrand factor-induced platelet P-Selectin translocation in a PI3K/Akt pathway-dependent manner. Front Cell Dev Biol 2021;9:642108. https://doi.org/10.3389/fcell.2021.642108.
[8] Henzler HJ. Particle stress in bioreactors. Adv Biochem Eng Biotechnol 2000;67:35–82. https://doi.org/10.1007/3-540-47865-5_2.
[9] Hoffmeister KM, Josefsson EC, Isaac NA, Clausen H, Hartwig JH, Stossel TP. Glycosylation restores survival of chilled blood platelets. 1531-4 Science 2003;301(5639). https://doi.org/10.1126/science.1085322.
[10] Italiano JE, Lecine P, Shivdasani RA, Hartwig JH. Blood platelets are assembled principally at the ends of proplatelet processes produced by differentiated megakaryocytes. J Cell Biol 1999;147(6):1299–312. https://doi.org/10.1083/jcb.147.6.1299.
[11] Ito Y, Nakamura S, Sugimoto N, Shigemori T, Kato Y, Ohno M, et al. Turbulence activates platelet biogenesis to enable clinical scale ex vivo production. e18 Cell 2018;174(3):636–48. https://doi.org/10.1016/j.cell.2018.06.011.
[12] Li Y, Fu J, Ling Y, Yago T, McDaniel JM, Song J, et al. Sialylation on O-glycans protects platelets from clearance by liver Kupffer cells. Proc Natl Acad Sci 2017;114(31):8360–5. https://doi.org/10.1073/pnas.1707662114.
[13] Lin M.-Y., Lin C.-S., Hu S., Chung W.-H. Progress in the Use of Platelet-rich Plasma in Aesthetic and Medical Dermatology. *J. Clin. Aesthetic Dermatol.* 2020;13(8):28–35.PMID: 33178379; PMCID: PMC7595356.
[14] Menter FR, Langtry R, Völker S. Transition modelling for general purpose CFD codes. Flow Turbul Combust 2006;77(1):277–303. https://doi.org/10.1007/s10494-006-9047-1.
[15] Mookerjee S, Foster HR, Waller AK, Ghevaert CJ. In vitro-derived platelets: the challenges we will have to face to assess quality and safety. Platelets 2020;31(6):724–30. https://doi.org/10.1080/09537104.2020.1769051.
[16] Moreau T, Evans AL, Vasquez L, Tijssen MR, Yan Y, Trotter MW, et al. Large-scale production of megakaryocytes from human pluripotent stem cells by chemically defined forward programming. Nat Commun 2016;7:11208. https://doi.org/10.1038/ncomms11208.
[17] Nakagawa Y, Nakamura S, Nakajima M, Endo H, Dohda T, Takayama N, et al. Two differential flows in a bioreactor promoted platelet generation from human pluripotent stem cell-derived megakaryocytes. Exp Hematol 2013;41(8):742–8. https://doi.org/10.1016/j.exphem.2013.04.007.
[18] Pallotta I, Lovett M, Kaplan DL, Balduini A. Three-dimensional system for the in vitro study of megakaryocytes and functional platelet production using silk-based vascular tubes. Tissue Eng Part C Methods 2011;17(12):1223–32. https://doi.org/10.1089/ten.tec.2011.0134.
[19] Pongerard A, Mallo L, Gachet C, de La Salle H, Lanza F, Strassel C. Leukodepletion filters-derived CD34+ cells as a cell source to study megakaryocyte differentiation and platelet formation. J Vis Exp JoVE 2021;(171)). https://doi.org/10.3791/62499.
[20] Qi Y, Tan S, Corbitt N, Urbanik C, Salibindla A, Ni R. Fragmentation in turbulence by small eddies. Nat Commun 2022;13:469. https://doi.org/10.1038/s41467-022-28092-3.
[21] Strassel C, Lanza F, Gachet C. On the way to in vitro platelet production. Front Med 2018;5:239. https://doi.org/10.1016/j.tracli.2018.07.005.
[22] Thon JN, Mazutis L, Wu S, Sylman JL, Ehrlicher A, Machlus KR, et al. Platelet bioreactor-on-a-chip. Blood 2014;124(12):1857–67. https://doi.org/10.1182/blood-2014-05-574913.
[23] Tilburg J, Becker IC, Italiano JE. Don't you forget about me(gakaryocytes). Blood 2022;139(22):3245–54. https://doi.org/10.1182/blood.2020009302.
[24] Trowbridge E.A., Martin J.F., Slater D.N., et al. The origin of platelet count and volume. Clin. Phys. Physiol. Meas. Off. J. Hosp. Phys. Assoc. Dtsch. Ges. Med. Phys. Eur. Fed. Organ. Med. Phys. 1984;5(3):145–170. DOI:10.1088/0143–0815/5/3/007.
[25] Verma R, Kumar S, Garg P, Verma YK. Platelet-rich plasma: a comparative and economical therapy for wound healing and tissue regeneration. Cell Tissue Bank 2022;10(12):1–22. https://doi.org/10.1007/s10561-022-10039-z.
[26] Zhao X, Alibhai D, Walsh TG, Tarassova N, Birol SZ, Williams CM, et al. Platelet generation from circulating megakaryocytes is triggered in the lung vasculature. bioRxiv 2021. https://doi.org/10.1101/2021.11.01.466743.